

Designing Manhole in Water Transmission Lines Using Flow3D Numerical Model

Azin Movahedi^{a*}, Ali Delavari^b and Massoud Farahi^c

^a M.Sc. Faculty of Civil Engineering, K.N. Toosi University of Technology, Tehran, Iran

^bB.Sc. Irrigation Engineering, Uremia University, The Manager of Water and Water Waste Installations Affairs of Moshaver Yekam Engineers Company, Tehran, Iran

^c B.Sc. Faculty of Mechanical Engineering, K.N. Toosi University of Technology, The Designer Expert in Moshaver Yekam Company, Tehran, Iran

Received 28 October 2015; Accepted 24 November 2015

Abstract

Using cascades and drops existing in flow path has a history of 3000 years. Particularly, Roman engineers employed stepped spillways with the same idea in several countries; however, there are few information about the hydraulic performance of aqueducts. Most of these channels have flat long cross sections with low torsions (variable slope) such that they can encompass cascade and steep spillways or dropshaft. Given that there are few studies conducted on dropshafts, the present paper attempted to discuss about such structures in flow path and water transmission lines as well as introducing the existing principles and relations and present, the obtained results of designing through Flow3D. The obtained error percentage was about 20% which is acceptable for numerical studies.

Keywords: Drop manhole, Vertical shaft, Projectile, Finite volume, Flow3D.

1. Introduction

In studies related to Roman structures, cost and time of implementing projects depended on various issues such as tunnels, piers, arcades, raised foundations, and siphon. Roman projects have been completed during 3 to 15 years with an average cost of 23 to 69 million dollars each kilometer. Their structures have been designed for low discharge flows (0.2-2 m³/s) and low longitudinal slopes (about 1-3 m each kilometer, on average) [1-4]. Their studies include the three following areas:

- Smooth sharp shots
- Stepped channels
- Cascades and dropshafts

Using the third alternative (dropshaft) as the main branch of their channel requires a certain science of engineering and is considered as new designs. Hydraulically, dropshafts includes the followings:

- The possibility of implementing vertical drop in balance of trade
- Kinetic energy dissipation of fluid flow
- Flow aeration

In the first case, dropshaft will allow the relation between two flat channels which are placed in various trades in a very short distance from each other. The second case of these structures' uses is kinetic energy dissipation of fluid flow which is used to optimize the performance of structures and prevent scouring and erosion of downstream

* Corresponding author: azin.movahedi@yekom.com

hydraulic structures [5, 6 and 7]. The third case is flow aeration which is used to prevent cavitation and corrosion of water duct. Figure 1 shows a schematic of dropshaft. Table 1 also presents a summary of Roman studies on water channels [8].

Table 1. A summary of Roman studies on water channels [2]

Steep Section (1)	Ref. (2)	Geometry (3)	Flow conditions (4)	Remarks (5)
Dougga aqueduct Oued Melah	[Ca]	B ~ 3.3 m b ~ 0.35 m (tunnel)	$\Delta H \sim 4$ to 5 m	Located downstream of 200-m long bridge, upstream of tunnel.
Vaugneray, Yzeron aqueduct Puit du Bourg	[Co1]	Rectangular dropshaft : h = 2.55 m, b = 0.4 m, B = 1.14 m, L = 1.9 m	$\Delta H = 21.9$ m $d_c \approx 0.24$ m (?) d/s flow conditions : d ~ 0.35 m, V ~ 1.33 m/s	Vaugneray branch of Yzeron aqueduct.
Recret/Grézieu-la-Varenne, Yzeron aqueduct Puit Gonttenoire	[Co1]	Rectangular dropshafts Square dropshaft : h = 2.55 m, b = 0.55 m, B = L = 1.18 m, P = 1.12 m	$\Delta H = 38$ m $d_c \approx 0.197$ m	Main branch of Yzeron aqueduct.
Puit-en-bas		Rectangular dropshaft : h = 2.5 m, b = 0.55 m, B = L = 1.17 m, D = 1.26 m, P = 1.35 m	$d_c \approx 0.197$ m d/s flow conditions : d ~ 0.15 m, V ~ 1.9 m/s	
Chabet Hlelouine, Chercell aqueduct Puit amont	[LP]	Circular dropshaft : h = 0.77 m, b = 0.94 m, $\phi = L = 2.03$ m, P > 1.75 m	$\Delta H = 12.28$ m Supercritical upstream flow : V ~ 8 m/s	4 series of steep chutes followed by circular dropshaft. Located downstream of steep smooth chute.
Gunugu aqueduct Moulin Romain	[LP]	Circular dropshaft : h ~ 3.5 to 4 m, b = 0.38 m, $\phi = L = 0.80$ m	$\Delta H = 20$ m	Upstream channel : 0.86-m wide.
Ruscade aqueduct	[Ve]	Circular dropshafts		
Beaulieu aqueduct Puit d'Olivari Puit du Château	[CQ]	Dropshaft : h = 6.2 m, b ~ 0.45 to 0.6 m Dropshaft : h ~ 8 m	$\Delta H = 37$ m	Combination of steep chutes and dropshafts. Rectangular or circular ? 147-m between dropshaft. Rectangular or circular ? 167-m between dropshaft.
Brisecou Forest, Montjeu aqueduct	[CQ, PR]	Rectangular dropshaft : h = 4.4 m, b = 0.8 m, B = 3.0 m, L = 2.4 m, D = 1.57 m, P > 0.8 m 9 dropshafts (h = 4.4 m) 15 dropshafts (h = 4.4 m)	$\Delta H \sim 140$ m x ~ 770 m	A series of 24 dropshafts (possible combination with steep chutes). 15 to 30-m between dropshaft. 50 to 120-m between dropshaft.
Cuicul aqueduct Grand thermes distribution line	[AI]	Circular (?) dropshafts: h ~ 1 to 0.4 m, b = 0.45 m, $\phi = L = 0.80$ m	$\Delta H \sim 3$ m x ~ 85 m	Series of 4 dropshafts on an urban distribution line.
Köln aqueduct Mechernich-Lessenich	[Gr]	Rectangular dropshaft : h = 0.35 m, b = 0.7 to 0.75 m, B = 0.9 m, L = 1.185 m, P = 0.2 m		[Gr, p. 97] One dropshaft installed along a steep section ($\Delta H \sim 84$ m, $\theta \sim 2.6^\circ$).
Valdepuentes aqueduct (Aqua Vetus), Cordoba	[Lop, Vi1, Vi2]			Several dropshafts and dropshaft cascades.
		One (?) dropshaft	$\Delta H = 3$ m	Homillo
		Dropshaft cascade : 34 dropshafts	$\Delta H \sim 120$ m x ~ 400 m	Cerro de los Pinos. Upstream of Valdepuentes bridge. Three unusual 90-degree bend shafts: <i>spiramina</i> . Shaft equipped with steps sculpted inside (h ~ 0.5 m).
		Pozo No. 11: circular dropshaft: h = 2.9 m, b = 0.6 m, $\phi = L = 0.61$ m, P = 0.76 m u/s slope : $\theta \sim 5\%$ d/s slope : $\theta \sim 5\%$		
		Pozo No. 21: circular dropshaft: h = 3.1 m, b = 0.5 m, $\phi = L = 0.55$ m, P = 0.9 m		90-degree bend shaft equipped with steps sculpted inside (h ~ 0.6 m).

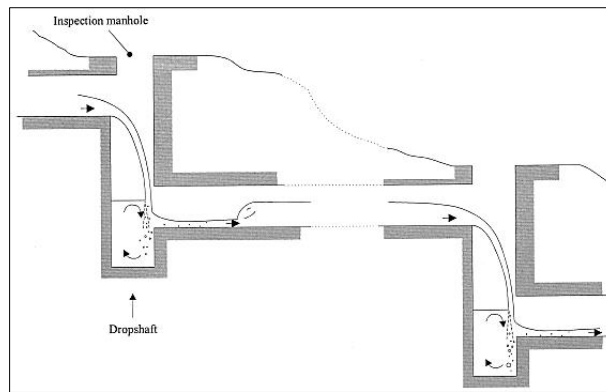


Figure 1. Schematic of drop manholes [1]

2. Introducing Flow Conditions in the Model

The purpose of the present study is to design a dropshaft which can be circular, rectangular or square. Since concreting square dropshaft is easier than concreting circular dropshaft, square dropshaft is the base of designing in the present paper. The height difference of upstream and downstream pipes (drop height) is 3 m and the diameter of upstream and downstream pipes is 1600 mm with the slope of 0.01 (1%).

Discharge of the design is $6 \text{ m}^3/\text{s}$. It is fed by its upstream spillway and falls into an open channel with the length of 18.5 m. The purpose of designing is to reach a state of flow regime which firstly, transmission lines pipes contain fluid as much as 75% of cross section (80% of the pipe diameter), i.e. flow is not under the pressure in the pipes; secondly, the length of dropshaft should be in such a way that the projected fluid jet from the upper pipe to the downstream wall have slight or no collision. The height of dropshafts, depending on the depth of burial in soil, is different and its other dimensions are implemented as tip across transmission line in 5 points of a 500-m-path. Finally, after passing this path by the fluid, transmission line and dropshafts are discharged into a river in downstream. Flow in the upstream of dropshaft and in conversions channel is supercritical and enters into the dropshaft with a normal depth of 20 cm, critical height of 51 cm (according to Eq. 1), velocity of about 4.5 m/s, and the slope of 0.02 (2%). Therefore, it can be stated that flow in pipe lines have supercritical flow which requires appropriate design to supply the objectives of the design. Figure 2 shows a schematic of hydraulic parameters used in the governing relations.

$$\text{Critical depth in rectangular channel: } d_c = \sqrt[3]{\frac{Q^2}{gb^2}} \tag{1}$$

Where d_c indicates critical depth of flow in the open channel (m); Q indicates flow discharge (m^3/s) and b indicates the width of channel (m) which is 8 m in this research.

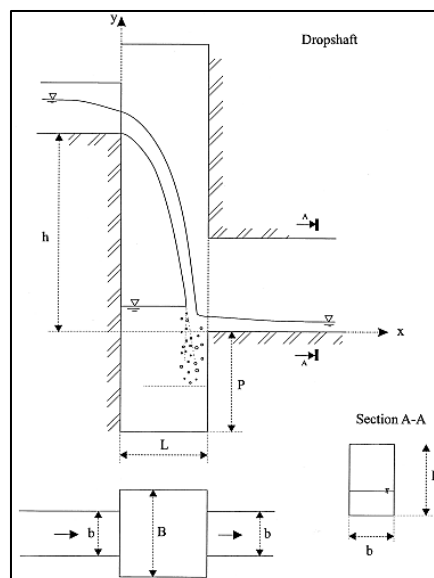


Figure 2. The employed parameters [1]

Selecting appropriate flow regime in designing is perform to prevent the collision of the jet projected to lower wall of dropshaft since the collision of this jet to the wall causes corrosion and destruction of the wall and disturbs the dropshaft use by the time pass. In the following, a schematic of various flow regimes has been presented:

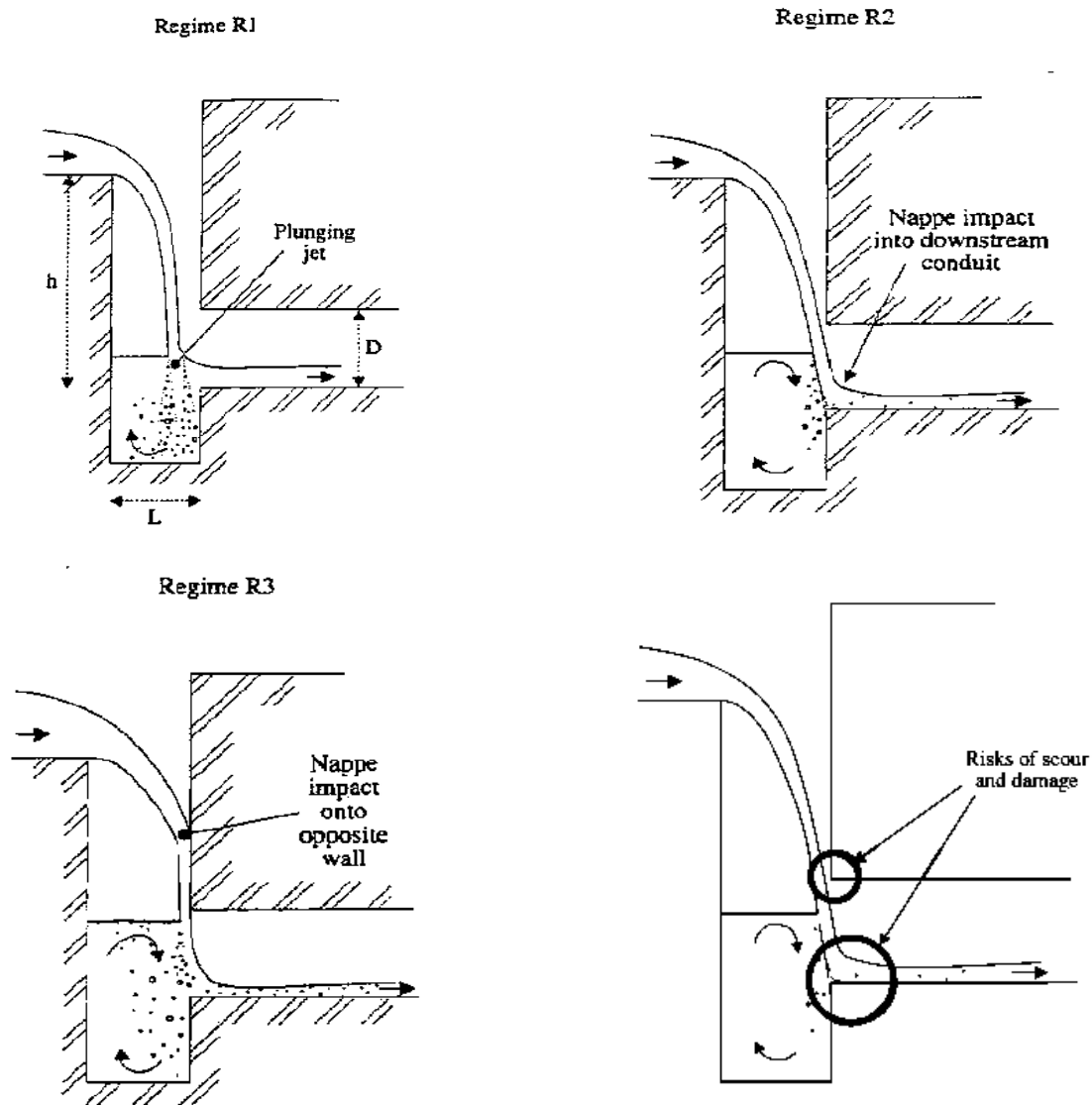


Figure 3. Various flow regimes and the place of projectile’s collision with the wall [1]

3. Relations Governing Flow

The relations which should be investigated in the present study are presented. To start computations, using the available relations, the primary dimensions for the dropshaft are assumed. After investigating the governing relations, the available model is simulated through Flow3D to compare the results. Selecting flow regime of R_1 , the relations are as following [2]:

$$0.035 \leq \frac{d_c}{L} \leq 0.15 \tag{2}$$

Where, L indicates length and width of the dropshaft (m).

Substituting the critical depth value, the length of the dropshaft will be (3.4 m and 14.5 m) considering affordability of the design; the length of the design is regarded 4.5 m. Since the best performance of the dropshaft for supercritical regimes is considered R_1 , for the accuracy of the primary assumption of the dropshaft length selection, the following control relation can be used [1]:

$$\frac{V_b}{\sqrt{g \cdot L}} < \frac{1}{2} \cdot \frac{h}{L} \cdot \left(\sqrt{8 \frac{L}{h} + \frac{Q^2}{gb^2h^2L}} - \frac{Q}{\sqrt{gb^2Lh^2}} \right) \tag{3}$$

Where V_b denotes the velocity of inlet flow in the dropshaft and H indicates the height of fluid drop (m). Other parameters have been previously introduced. Substituting the study dimensions in Eq. 3, heterogeneity assumption is established, confirming the accuracy of the primary assumption in the dropshaft's dimensions selection. Another important dimension is p value which can be extracted from the next graph:

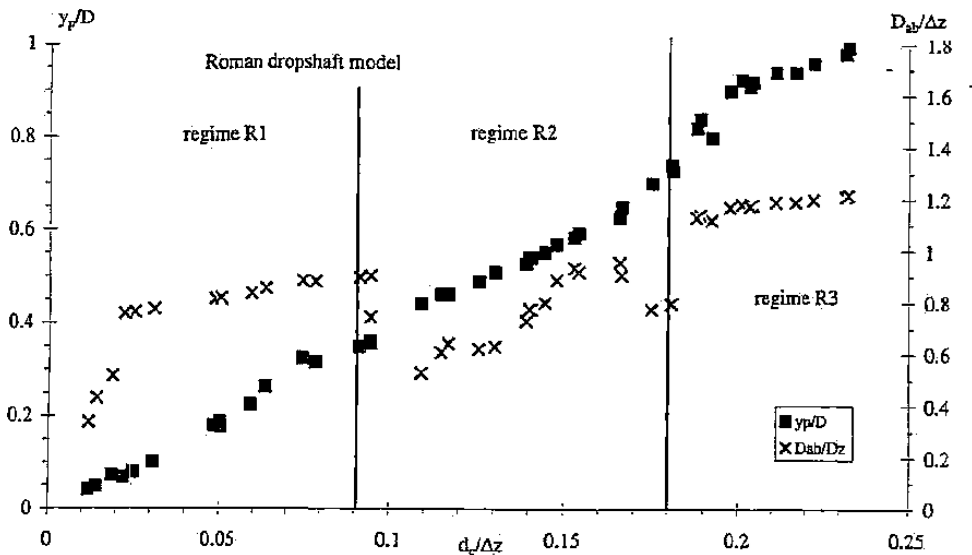


Figure 4. The non-dimensionalized height of the dropshaft relative to d_c/h and D_{ab}/h

Since the 80% of the lower pipe's diameter should be filled with fluid, thus $y_p/D = 0.8$. Given to Figure 2, it is clear that $D_{ab} = p + y_p$. Accordingly, p is considered 1.7 m. Therefore, the dropshaft has been designed with the length and width of 4.5 m and the height (p) of 1.7 m. These dimensions should be simulated by Flow3D to confirm flow model in the pipe and manhole.

4. Flow3D Numerical Model

In Flow3D model, the equations governing fluid flow includes continuity and momentum equations. Flow continuity equation is obtained from the law of conservation of mass as well as by writing mass balance equation for compressible and viscous fluid simple element. In general, this equation is written as following:

$$V_F \frac{\partial \rho}{\partial t} + \frac{\partial}{\partial x}(\rho u A_x) + \frac{\partial}{\partial y}(\rho v A_y) + \frac{\partial}{\partial z}(\rho w A_z) = 0 \tag{4}$$

Where V_F indicates the ratio of the volume of the fluid passing through an element to total volume of the element and ρ denotes the density of the element. Velocity components (u, v, w) are in (x, y, z) directions. A_x indicates the ratio of the area of the fluid passing through an element to total area of the element at the direction of x . A_y and A_z , similarly, are flow levels at the directions of y and z . Navier-Stokes equations of fluid with velocity components of (u, v, w) have been shown in 3-dimensional coordinates:

$$\begin{aligned} \frac{\partial u}{\partial t} + \frac{1}{V_F} \left\{ u A_x \frac{\partial u}{\partial x} + v A_y \frac{\partial u}{\partial y} + w A_z \frac{\partial u}{\partial z} \right\} &= -\frac{1}{\rho} \frac{\partial P}{\partial x} + G_x + f_x \\ \frac{\partial v}{\partial t} + \frac{1}{V_F} \left\{ u A_x \frac{\partial v}{\partial x} + v A_y \frac{\partial v}{\partial y} + w A_z \frac{\partial v}{\partial z} \right\} &= -\frac{1}{\rho} \frac{\partial P}{\partial y} + G_y + f_y \\ \frac{\partial w}{\partial t} + \frac{1}{V_F} \left\{ u A_x \frac{\partial w}{\partial x} + v A_y \frac{\partial w}{\partial y} + w A_z \frac{\partial w}{\partial z} \right\} &= -\frac{1}{\rho} \frac{\partial P}{\partial z} + G_z + f_z \end{aligned} \tag{5}$$

In these equations, (G_x, G_y, G_z) are the terms of mass acceleration and (f_x, f_y, f_z) are the terms of viscous acceleration [10 and 11]. To numerically simulate the equations governing these flows, Flow3D is employed. Flow3D is powerful software in CFD area. Flow3D has been designed for 1-2-3 dimensional problems. One of the main advantages of this software for hydraulic analyses is the ability of modeling flows with free surface. Free surface refers to the interval between gas and liquid. Free surface is simulated using Volume of fluid (VOF) [12]. Flow environment is divided into networks with fixed rectangular cells such that for each cell, there are average values of dependent quantities. On other words, all variables are computed at the center of the cell except that velocity which is computed at the center of cell faces. In this software, two numerical techniques have been used for geometrical simulation [10].

1. Volume of fluid (VOF) method: it is used to show the behavior of fluid at free surface and includes the following three components [13]:

- Displaying the position of surface
- Meshing
- Boundary conditions of surface

2. Fractional Area-Volume Obstacle Representation (FAVOR): it is employed to simulate surfaces and rigid volumes such as geometrical boundaries. For numerical modeling, turbulence numerical model is required. In Flow3D, for this purpose, five turbulence models have been introduced including: Prandtl's Mixing Length, $k-\epsilon$ one and tow-equations, RNG models, and Large Eddy Simulation Model. RNG-based models less rely on constant empirical figures. RNG model uses equations which are similar to $k-\epsilon$ turbulence model equations. Constant values of the equation which have been practically received in the standard mode of $k-\epsilon$ have been taken from RNG. The presence of an additional term in the equation ϵ causes the increase of computations accuracy in strain flow in RNG model. RNG, compared to standard $k-\epsilon$ model, has a higher efficiency in strain flow; and unlike the standard model, analytical relation is used to determine Prandtl turbulence figures. Therefore, this model has an appropriate accuracy in low Reynolds numbers and it is more considered to determine turbulence values of flow in curved fields or geometrical complexity [14]. Accordingly, RNG has been used in the present study.

5. Simulation Results

In this section, the rigid model constructed in Solidworks 2011 software is referred. Then, its geometrical meshing and Boundary conditions are discussed. Finally, the obtained results are presented. In this model, three meshing blocks have been selected. The first block pertains to conversion channel at upstream with the length of 18.5 m. in inlet section of channel, volume flow rate with the discharge of $6 \text{ m}^3/\text{s}$ and outlet section has symmetry Boundary conditions. Other faces also have wall Boundary conditions. The second block which encompasses dropshaft has symmetry condition in inlet and outlet sections and walls have been also defined. The third block which encompasses about 14 m of transmission line has symmetry inlet and outlet Boundary conditions as well as other conditions of wall. The following figure shows Boundary conditions:

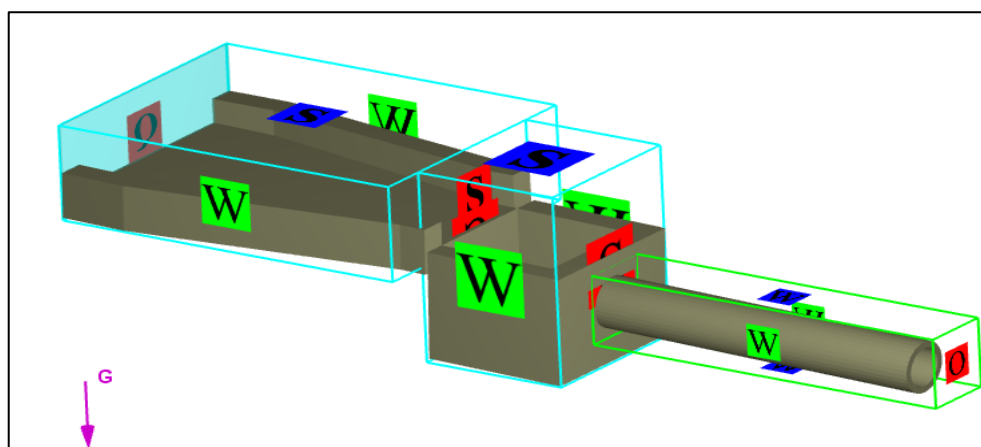


Figure 5. The Boundary conditions applied to the numerical model

After selecting appropriate dimensions of meshing and obtaining steady flow, the extracted numerical results are investigated, the following diagrams show steady flow state in which flow reaches a balance and does not change after 40 sec. These figures indicate that simulation time for this study has been appropriately selected (80 sec) and it can also be decreased to 45 sec.

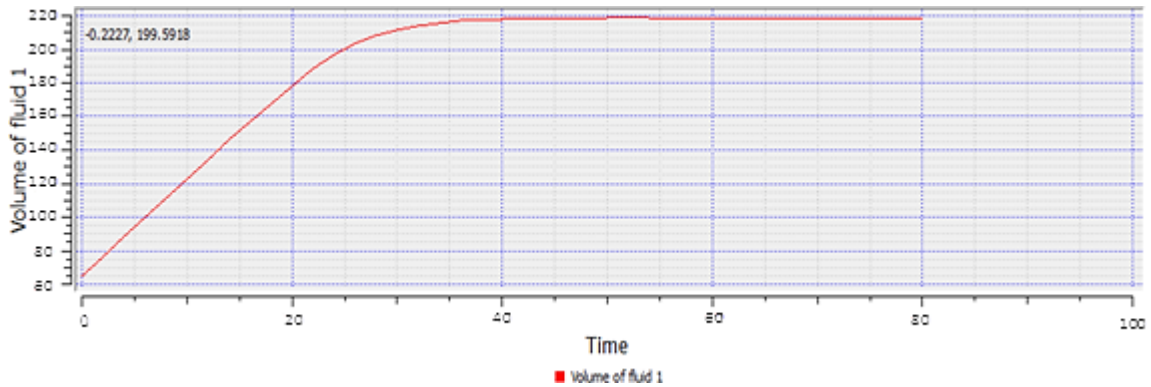


Figure 6. The diagram of fluid volume and flow stability by the time pass

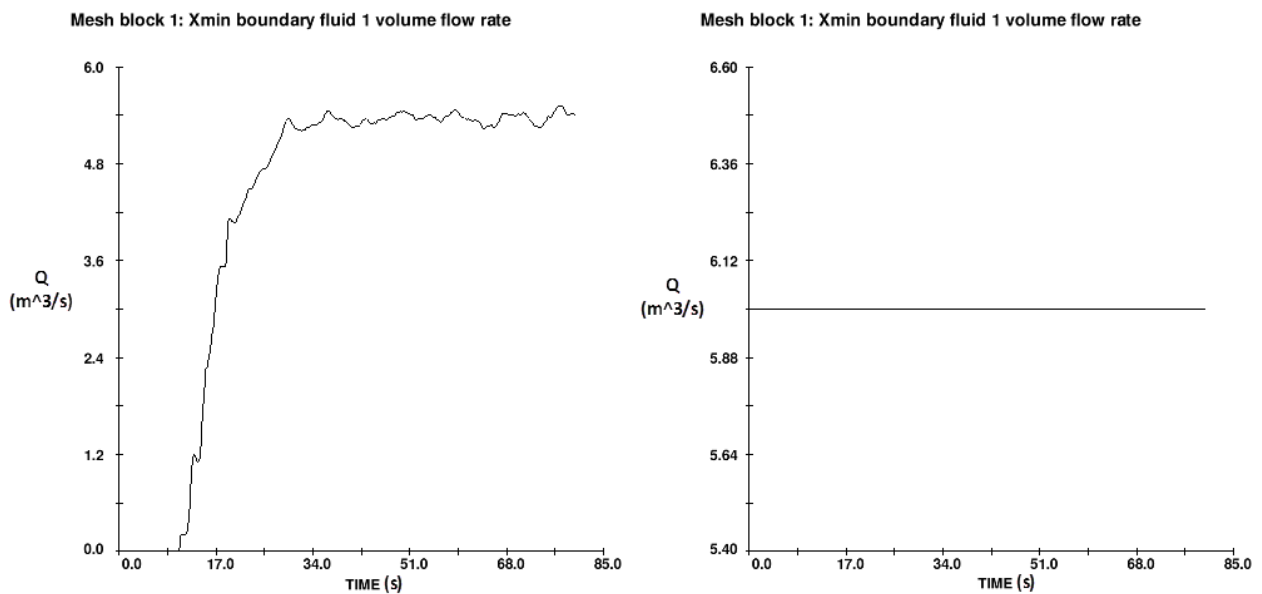


Figure 7. Diagram of inlet and outlet flow passing through Boundaries by the time pass; inlet Boundary (right) and outlet Boundary (left)

Selecting appropriate dimensions of meshing cells causes that the curvatures of the rigid model are well modeled and the rigid model is closer to the real states (the simulation accuracy is increased). Figure 8 shows a schematic of FAVOR method to observe the rigid model after meshing which indicates its closeness to real geometry model.

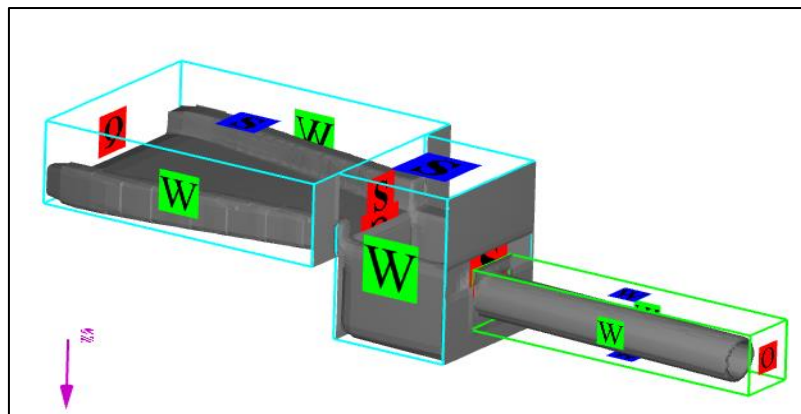


Figure 8. FAVOR method in modeling the rigid model geometry

In the following figures, flow pattern and hydraulic parameters (depth, velocity, and Froude number) in transmission line are presented:

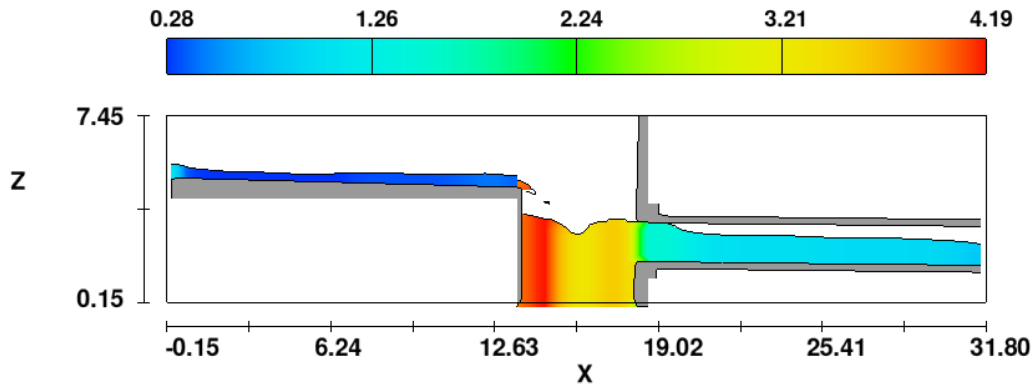


Figure 9. Flow depth at final moment of numerical simulation

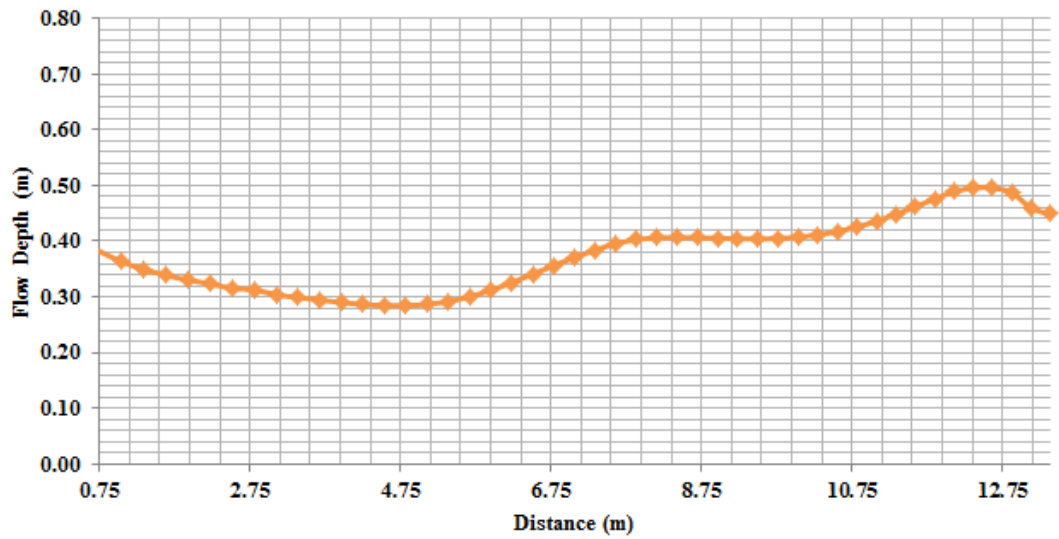


Figure 10. Flow depth in transmission channel (upstream)

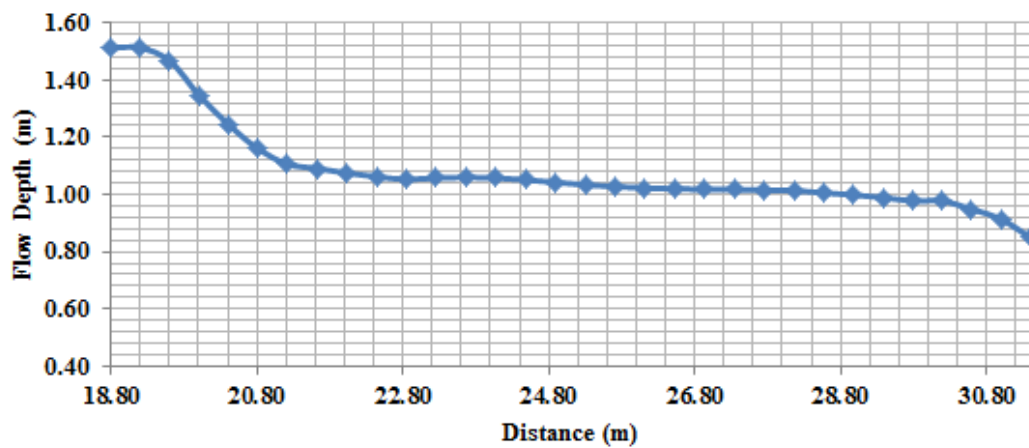


Figure 11. Flow depth in downstream pipe

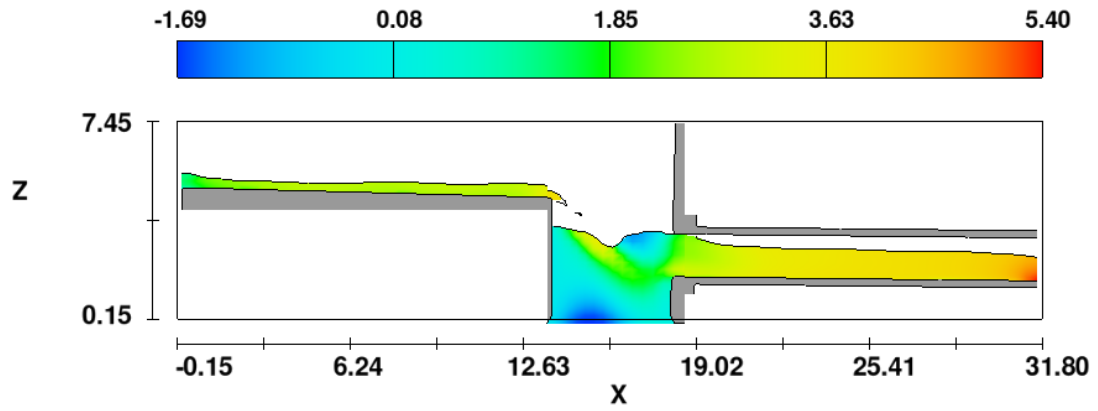


Figure 12. Flow velocity at the final moment of numerical simulation

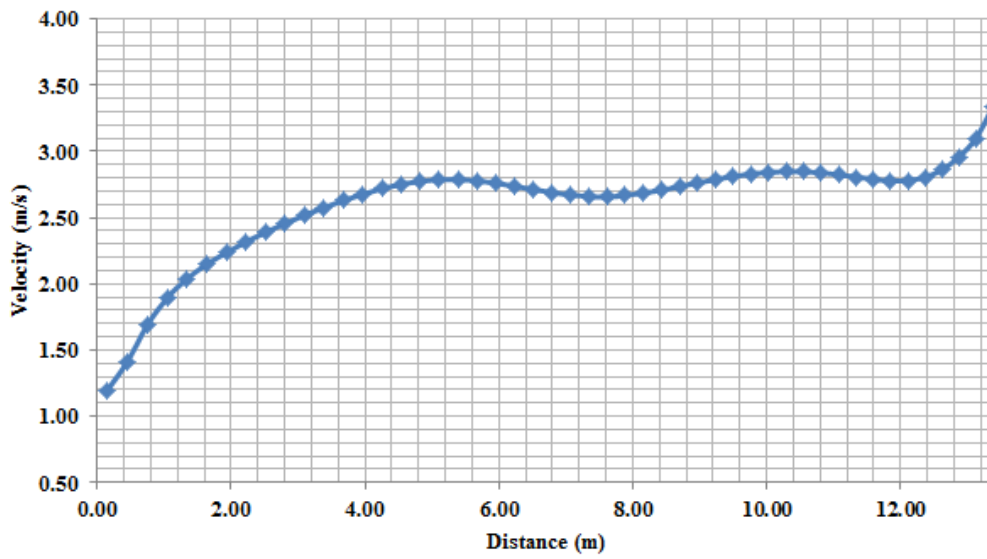


Figure 13. Flow velocity in transmission channel (upstream)

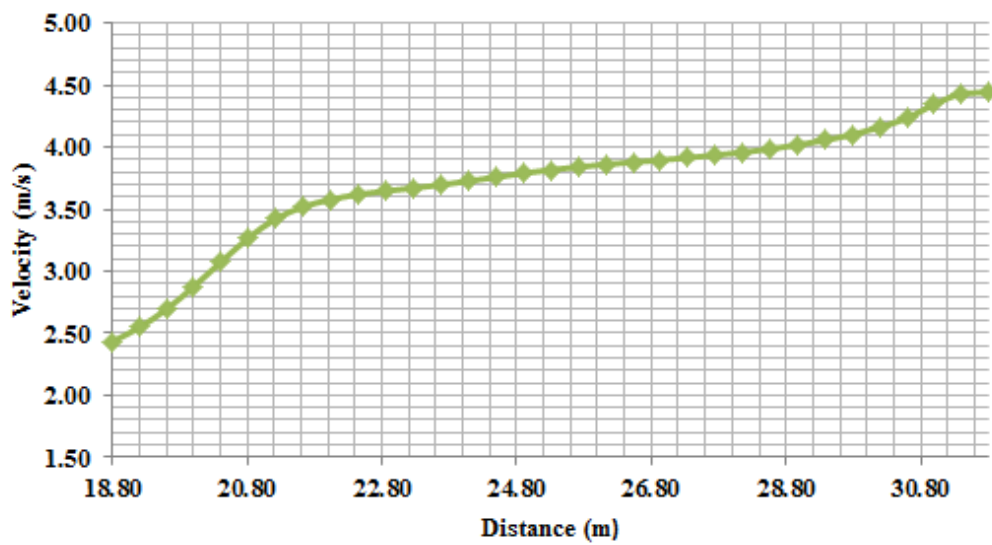


Figure 14. Flow velocity in downstream pipe

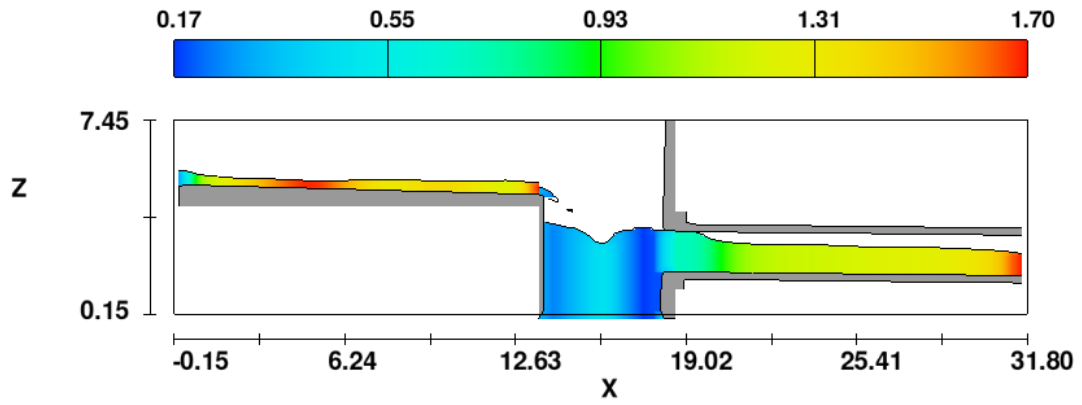


Figure 15. Froude number at the final moment of numerical simulation

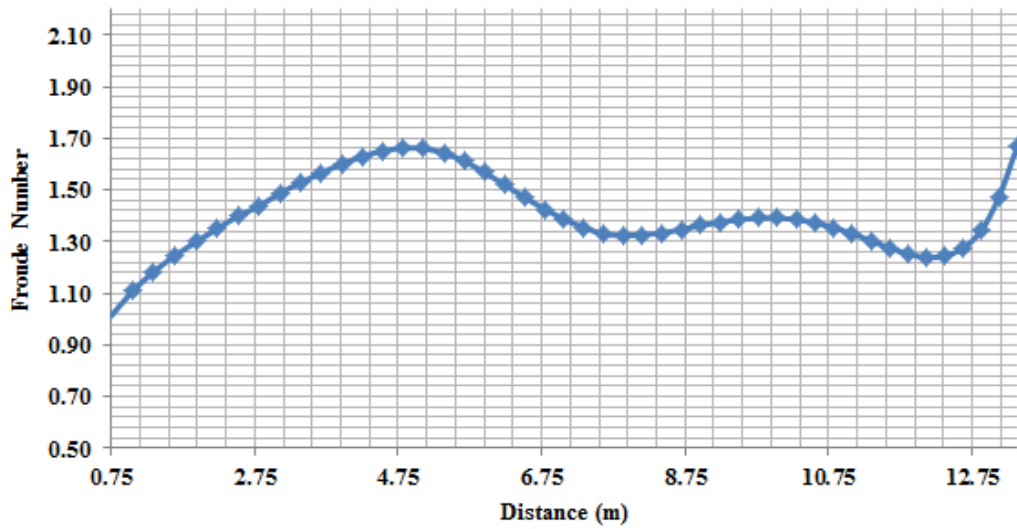


Figure 16. Froude number in transmission channel (upstream)

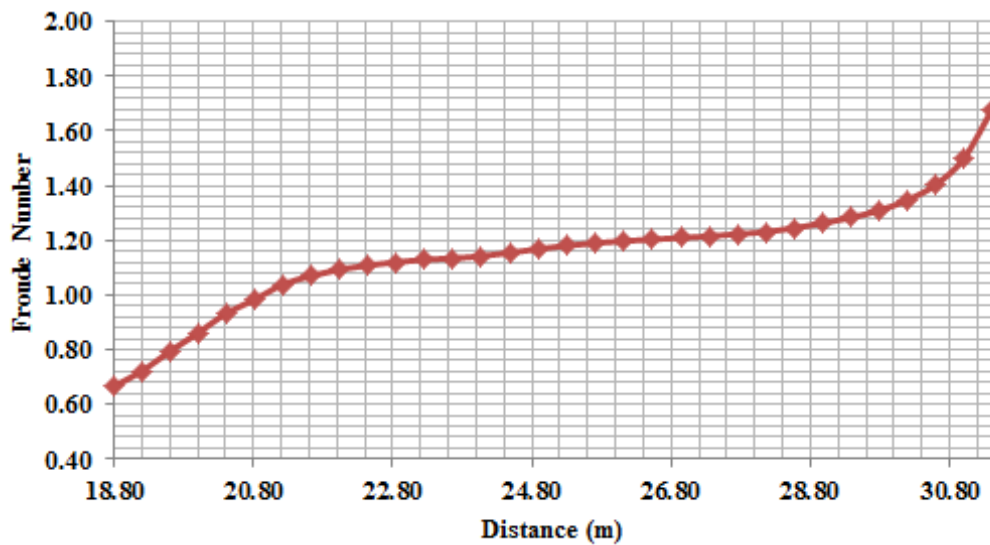


Figure 17. Froude number in downstream pipe

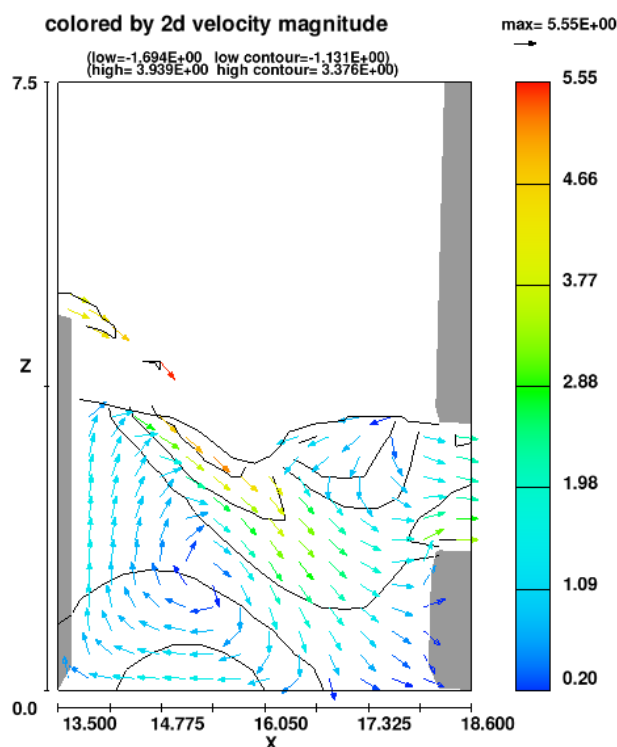


Figure 18. Schematic of size and direction of velocity vectors in drop manhole

Considering Figures 9 to 17, it is revealed flow pattern has a supercritical trend which flows with a relatively constant and stable depth in upstream channel. After entering into the dropshaft, this flow pattern with its relatively high velocity firstly causes flow obstruction in the beginning of the pipe and then, exists from downstream pipe with free surface flow states. The depth and velocity of the flow in the model is very close to the manually computed value and it has an error percentage of below 20% (this value is acceptable in numerical studies up to 30% and numerical results can be relied on to reach these values). Additionally, in the model, there is no trace of projectile jet collision from the upstream channel to downstream wall. It can be stated that flow regime of R_1 is established in the model and the structure damage is in its minimum state. Finally, it can be said that the dimensions which have been selected from manual computations method for this design are acceptable values and the design can be confirmed.

6. Conclusion

In the present paper, using relations available in other researches, a drop manhole was designed in downstream water transmission line of a spillway by formulating the considered research hypotheses and objectives. Then, using Flow3D, the dropshaft with the height of 3 m and discharge of $6 \text{ m}^3/\text{s}$ was simulated to extract its flow and hydraulic parameters. The extracted parameters have been well consistent with manual computations values. The obtained error percentage was about 20% which is acceptable for numerical studies. Figures, flow pattern and hydraulic parameters were also presented.

7. References

- [1] Chanson, Hubert. "Hydraulics of Roman aqueducts: steep chutes, cascades, and dropshafts." *American Journal of Archaeology* (2000): 47-72.
- [2] Chanson, Hubert. "Hydraulic design of stepped cascades, channels, weirs and spillways." (1995): 1-292.
- [3] Fevrier, P.A. "The Roman Army and the Construction of Aqueducts." (1979).
- [4] Hodge, A. T., Roman Aqueducts, and Water Supply. "Duckworth." London, United Kingdom (1992).
- [5] Jain, Subhash Chandra, and John Fisher Kennedy. Vortex-flow drop structures for the Milwaukee metropolitan sewerage district inline storage system. Iowa Institute of Hydraulic Research, the University of Iowa, 1983.
- [6] Apelt, C. J. "Goonyella railway duplication drop structures and energy dissipators at culvert outlets. Model studies." Report

CH27 84 (1984).

- [7] Rajaratnam, N., A. Mainali, and C. Y. Hsung. "Observations on flow in vertical dropshafts in urban drainage systems." *Journal of Environmental Engineering* 123, no. 5 (1997): 486-491.
- [8] Ervine, D. A., and A. A. Ahmed. "A Scaling relationship for a two-dimensional vertical dropshaft." In *Proc. Intl. Conf. on Hydraulic Modelling of Civil Engineering Structures*, pp. 195-214. 1982.
- [9] Chanson, Hubert. "Energy dissipation and drop structures in ancient times: the Roman dropshafts." In *Water 99 Joint Congress, 25th Hydrology & Water Resources Symposium and 2nd International Conference on Water Resources & Environmental Research*, vol. 2, pp. 987-992. 1999.
- [10] Hoseini, A. and Abdipour, A. Numerical modeling of velocity profile in continuous muddy flows and investigating the effect of slope, concentration and discharge on the flow. *Civil engineering magazine of Azad Islamic University*, the 3rd year, no. 3. (2010).
- [11] Flow Science. "FLOW-3D User's Manuals Version 9.2.1." Flow Science, Inc., Los Alamos, New Mexico, USA. (2008).
- [12] Baghdadi, H.; Ershadi, S. and Rostami, M. Numerical investigation of topical scouring due to sought horizontal directions using Flow3D. *The 10th Iranian hydraulic conference*, Gilan University. (2011).
- [13] habibi, M. and Khanjani, M. J. Investigating scouring phenomenon in long vertical shoap drop and comparing laboratory model with the results obtained by Flow3D, the 8th international congress on civil engineering, Shiraz University. (2009).
- [14] Movahedi, A.; Kavianpour, M. R. and Aminoroayayi Yamini, A. Nurmerical analysis of downstream scouring hole of cup launchers using Flow3D, *international conference on civil engineering, architecture and sustainable development*, Tabriz. (2013).